

Simultaneous Control of inside Air Temperature and Humidity by coupled Heating and Ventilation in a Greenhouse

Hafidha Maouel^{1,*} and Said Makhlof²

¹Laboratory of thermodynamic and energetic systems, Houari Boumediene university, BP 32 El Alia, 16111, Algiers, Algeria.

² L.M.S.E. Laboratory, Department of Mechanics, Mouloud Mammeri university, Faculty of Construction, Po 15000, Tizi Ouzou, Algeria.

*Corresponding Author: Maouel Hafidha. Email: h.maouel@usthb.dz

ABSTRACT: Greenhouse ventilation combined with heating is required to control temperature and moisture levels for a comfort and provide CO₂ for good photosynthesis. The present study focuses on the simulation of a climate in greenhouse during winter. The mathematical model, based on the energy and the water vapor balances inside the greenhouse is used. The main equations of flow are solved with the Fluent[®] CFD package inside and outside the greenhouse. The external conditions are those of Mediterranean climate and the greenhouse is located in Tizi-Ouzou (Algeria). The study aims at getting a better compromise between flow heating combined with the air exchange rate (a technique used for the dehumidification of the air). After describing the physical phenomena, the equations that govern these phenomena and the method of solving these equations, a program for calculating the inside temperature and humidity was developed and validated by comparison with simulation results. To simulate turbulence inside and outside greenhouse the $k-\varepsilon$ Standard turbulence model, which comes out (seems) to be more accurate than the other models, have been preferred. Analytical results are used to determinate optimal conditions of flow heating combined with ventilation rate.

KEYWORDS: Greenhouse; Plants; Heating; Natural ventilation; CFD.

1 Introduction

The greenhouse is a very complex biological and energy system in which most of the modes of heat and mass transfer are brought into play in a confined environment. Many physical and biological mechanisms cannot be described with good accuracy, because a large number of parameters are involved. The micro-climate which prevails in the greenhouse is the result of the meteorological inputs, the thermodynamic properties of the elements emitting water vapor (soil and vegetal) and the influence of artificial systems of climate control (such as heating and cooling systems). Consequently, the heat flow is transferred by: i) conduction through the soil, ii) convection on the surface of the cover, plants and soil (and possibly exchangers), iii) evaporation from the soil and plants and condensation on the cover and foliage. These exchanges are also due to the air motions, caused by the greenhouse permeability or by forced ventilation. As the cover may be considered an enormous solar collector, the solar radiation gain through the roofing material must be added to the radiation exchanges of long wavelength between different elements. The complexity of the model is not only related to the diversity of considered physical phenomena taken into account the energy balance but it also comes from the complicated mathematical formulation of some natural processes, for which the equations are often nonlinear. However, there is no general analytical method to solve these systems. For this type of problems, the use of numerical methods is essential, as far as the use of calculators. In recent years, several studies on climate and air flow in greenhouses were performed and have yielded significant results (Haxaire, 1999[1]; Boulard, 2010[2]; Roy, 2002[3]; Lee, 2000[4] and Edwin et al 2019 [5]).

The present study which complements the previous works deals with the ventilation of greenhouses through openings as a means of controlling the greenhouse climate parameters allows among others to:

- regulate the greenhouse air temperature.

46 - limit especially the inside moisture to reduce or eliminate the fungal diseases development such as
 47 botrytis,
 48 - provide the carbon dioxide to the plants by the renewal air.

49 One of the roles of ventilation system is to eliminate excess inside humidity. If not properly vented,
 50 excess humidity condenses on the leaf surface where it can enhance disease problems (Badia 2021[6]). It
 51 can also condense on the greenhouse cover where it can reduce light transmission. Such, the plants were
 52 penalized of solar heating. Greenhouse humidity levels can be reduced by removing the moist air around the
 53 plants and replacing it with the cooler and drier outside air(Zhong et al 2022[7]).

54 It is known that high relative humidity is undesirable for growing most greenhouse plants. It is one of the
 55 major contributing factors to a variety of plant diseases, including a trio of damping-off diseases and
 56 Botrytis blight, a common fungal disease of bedding plants (Boulard, 2002[8]).

57 This study focuses to reduce relative humidity using a combined heating and ventilation. To perform
 58 this study, the air motions in an unheated greenhouse with plants inside, was simulated in numerically for
 59 different openings. Thereafter, in order to make a comparison with a heated greenhouse, other simulations
 60 were conducted in this case. Thus the convection loops inside the greenhouse, the temperature profiles
 61 and velocities for the various configurations, taking into account the combined effect of vegetation (both
 62 as a source of steam and sink of heat), were determined. The main purpose of this study is obviously to
 63 control humidity by heating combined with air motions, so as to get a compromise between the heating
 64 and ventilation that is covered here.

65 2 Theory/calculation

66 2.1 Water vapour balance

67 The water vapour can be expressed, in permanent regime, by the following equation which reflects that,
 68 the water vapour produced by the vegetal is exchanged with outside air:

$$70 h_m LAI_S (w_{(T_V)}^{sat} - w_a) = \rho_a N h_0 (w_a - w_e) / 3600 \quad (1)$$

72 2.2 Greenhouse energy balance

73 As the heat storage term is smaller than the other fluxes, it is neglected in this case and we can write:

$$75 \eta R_{ge} + HP = (T_a - T_e) [K_c S_c / S_{sol} + \rho_a C p_a N h_0 / 3600] + (w_a - w_e) \rho_a L_v N h_0 / 3600 \quad (2)$$

77 2.3 Crop energy balance

78 The temperature of the leaf of vegetal does not represent effectively the physiological behavior of the
 79 culture. Foliage temperature (T_v), which depends on transpiration, is a much more appropriate control
 80 parameter. The T_v temperature is therefore estimated by the following equation which reflects that, the heat
 81 radiation received by the crop is transferred to the ambient air by sensible and latent heat:

$$83 \alpha T R_{ge} = 2 h_a LAI_S (T_v - T_a) + h_m LAI_S L_v (T_v) (w_{(T_V)}^{sat} - w_a) \quad (3)$$

85 The solving of the above system of equations, gives for the three variables (w_a , T_a and T_v):
 86 Ambient moisture content is given by:

$$88 w_a = [h_m LAI_S L_v (T_v) w_{(T_V)}^{sat} + \rho_a N h_0 w_e / 3600] / [h_m LAI_S + \rho_a N h_0 / 3600] \quad (4)$$

89 Ambient air temperature is given by:

$$91 T_a = T_e + [\eta R_{ge} + HP - \rho_a N h_0 L_v (w_a - w_e) / 3600] / [K_c S_c / S_{sol} + \rho_a N h_0 C p_a / 3600] \quad (5)$$

93 Foliage temperature is given by:

$$94 \quad 95 \quad T_v = T_a + [\alpha\tau R_{ge} - h_m LAI_S L_v(T_v)(w_{(T_v)}^{sat} - w_a)]/2h_a LAI_S \quad (6)$$

96 Where:

97 N , the air exchange rate,
 98 η , the solar heating efficiency estimated of 0.65 for single cover (Boulard et al 1993[9])
 100 τ , the greenhouse global transmission,
 101 α , the canopy absorption coefficient for solar radiation,
 102 R_{ga} , the global radiation absorbed by vegetal: $R_{ga} = \alpha\tau R_{ge}$ where α is the canopy
 103 absorption coefficient for solar radiation and τ the greenhouse global transmission.

105 2.4 CFD Model

106 The modeling of fluid flow is to determinate the flow variables at any point and at every moment, the
 107 following representative flow variables:

- 108 - pressure p ,
- 109 - density ρ ,
- 110 - velocity vector \vec{v} and its three components,
- 111 - temperature T ,
- 112 - concentration C_i of different gases (water vapor and CO_2), which was not included in this study.

113 To simplify the problem, acceptable assumptions were adopted, which are:

- 114 - the fluid is Newtonian,
- 115 - the Boussinesq approximation is adopted,
- 116 - the volume forces are due only to the acceleration of gravity,
- 117 - the fluid is completely transparent for the radiation flux (no absorption coefficient for radiation
 118 $abs=0$).

119 To establish the governing equations, we use the conservation principles of mechanics and
 120 thermodynamics. Thus, we can write the conservation equations of: i) mass, ii) momentum quantity
 121 (vector equation equivalent to three scalar equations) and iii) energy. For this system of equations, the
 122 equation of mass transfer (relative to water vapor) is added in the case of binary mixtures. Finally, we
 123 obtain the following system of equations traducing the conservation principles of mechanics and
 124 thermodynamics:

$$125 \quad 126 \quad 127 \quad \left\{ \begin{array}{l} \vec{\nabla} \vec{V} = 0 \\ \frac{\partial \vec{V}}{\partial t} + \vec{V} \vec{\nabla} (\rho \vec{V}) = -\frac{1}{\rho} \vec{\nabla} p + \vec{v} \Delta \vec{V} \\ \frac{\partial T}{\partial t} + \vec{V} \vec{\nabla} (T \vec{V}) = \frac{\lambda}{\rho C_p} \Delta T + \frac{q}{\rho C_p} = a \Delta T + \frac{q}{\rho C_p} \\ \frac{\partial \omega}{\partial t} + \vec{V} \vec{\nabla} (\omega \vec{V}) = D_w \Delta \omega + S_w \end{array} \right\} \quad (7)$$

129 2.4.1 Turbulence Modeling

130 Even if it turns out that the equations presented above are representative of the instantaneous move-
 131 ments for a turbulent regime, current means of calculation and way of the presenting the results do not yet
 132 allow a direct turbulence simulation and the discrete method of resolution used pose major problems. In
 133 fact, it is impossible to simulate eddies whose size is less than one mesh. For all these reasons, we are led to
 134 adopt a statistical approach to turbulence which is that of Reynolds. A simplified approach based on the

135 statistical decomposition of the turbulent flow into an average and a fluctuating component (Reynolds
 136 decomposition) is considered. To account for the effects of turbulence, we opt for the standard model $k-\varepsilon$,
 137 which is more appropriate for this type of problems with a large boundary layer (Nebali, 2006) [10].

$$\left\{
 \begin{array}{l}
 \frac{\partial \bar{v}_j}{\partial x_j} = 0 \\
 \frac{\partial \bar{v}_i}{\partial t} + \bar{v}_j \frac{\partial \bar{v}_i}{\partial x_j} = -\frac{1}{\rho} \frac{\partial \bar{p}}{\partial x_i} + \frac{\partial}{\partial x_i} \left(\vartheta \frac{\partial \bar{v}_i}{\partial x_j} - \bar{v}'_i \bar{v}'_j \right) + F_i \\
 \frac{\partial \bar{T}}{\partial t} + \bar{v}_j \frac{\partial \bar{T}}{\partial x_j} = \frac{\partial}{\partial x_j} \left(a \frac{\partial \bar{T}}{\partial x_j} - \bar{v}'_j \bar{T}' \right) + \frac{q}{\rho C_p} \\
 \vartheta_t = C_\mu \frac{k^2}{\varepsilon} \\
 \frac{\partial \bar{k}}{\partial t} + \bar{v}_j \frac{\partial \bar{k}}{\partial x_j} = \frac{\partial}{\partial x_j} \left((\vartheta + \frac{\vartheta_t}{\sigma_k}) \frac{\partial \bar{k}}{\partial x_j} \right) - \bar{v}'_i \bar{v}'_j \frac{\partial \bar{v}_i}{\partial x_j} - \varepsilon + S_{k,p} \\
 \frac{\partial \bar{\varepsilon}}{\partial t} + \bar{v}_j \frac{\partial \bar{\varepsilon}}{\partial x_j} = \frac{\partial}{\partial x_j} \left[(\vartheta + \frac{\vartheta_t}{\sigma_k}) \frac{\partial \bar{\varepsilon}}{\partial x_j} \right] + \frac{\varepsilon}{k} \left[C_{1\varepsilon} \left(-\bar{v}'_i \bar{v}'_j \frac{\partial \bar{v}_i}{\partial x_j} \right) - C_{2\varepsilon} \varepsilon \right] + S_{\varepsilon,p} \\
 \frac{\partial \bar{\omega}}{\partial t} + \bar{v}_j \frac{\partial \bar{\omega}}{\partial x_j} = \frac{\partial}{\partial x_j} \left(D_\omega \frac{\partial \bar{\omega}}{\partial x_j} - \bar{v}'_i \bar{\omega}' \right) + S_{\omega,p}
 \end{array}
 \right\} \quad (8)$$

139 Compared to the steady state, the additional unknowns appear in the system of Equ. 8 where the five
 140 empirical constants of this model are the values presented in Table

141 **Table 1:** $k-\varepsilon$ model constants

Constant	Value
C_{1z}	1.44
C_{2z}	1.92
C_μ	0.09
σ_k	1
σ_z	1

142
 143 To this system of equations (8) is associated the Boussinesq relations written as follows:

$$\bar{v}'_i \bar{v}'_j = -v_i \left(\frac{\partial \bar{v}_i}{\partial x_j} + \frac{\partial \bar{v}_j}{\partial x_i} \right) - \frac{2}{3} \left(v_i \frac{\partial \bar{v}_j}{\partial x_j} - k \right) \delta_{i,j} \quad (9)$$

$$\bar{v}'_i \bar{T}' = -a_t \frac{\partial \bar{T}}{\partial x_i} = -\frac{v_t}{Pr_t} \frac{\partial \bar{T}}{\partial x_i} \quad (10)$$

146 $\overline{v'_i \omega} = -D_{\omega t} \frac{\partial \bar{\omega}}{\partial x_i} = -\frac{v_t}{s c_t} \frac{\partial \bar{\omega}}{\partial x_i}$ (11)

147

148 *2.4.2 Presence of vegetation in greenhouse*

149

150 The pressure drop through the stand of vegetation is modeled using the Forchheimer equation (Bruse,
151 1998), which calculates the pressure drop in porous media using the following equation:

152

153 $\Delta p = \frac{C_f}{\sqrt{k_p}} \rho \parallel \vec{v} \parallel \vec{v}$ (12)

154 k_p is the intrinsic permeability of the medium and C_f , the coefficient of nonlinear loss charge, which is introduced for
155 stand of tomato's leaves (Boulard et al., 1991).

156

157 *2.4.3 Energy balance equation for vegetation*

158

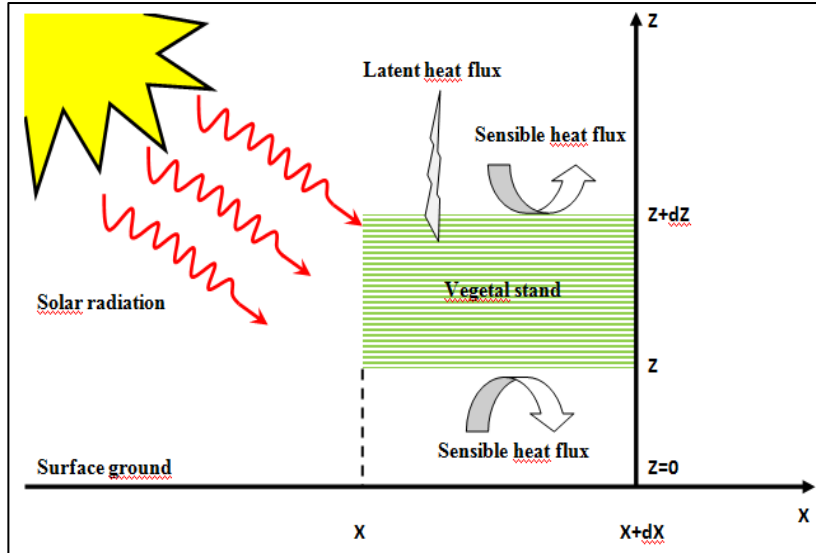
159 For the stand of vegetation as shown in fig. 1, the energy balance in permanent regime is given by:

160

161 $dR(z)/dz - LAI_V LvE - 2LAI_V C = 0$ (13)

162

163 Where $dR(z)/dz$ is the incident irradiative flux, $LAI_V LvE$, the heat latent flux, $2LAI_V C$, the sensible heat flux and
164 LAI_V , the volumetric leaf index given by: $LAI_V = LAI_S \cdot S_{sol}/Vol$.



179 **Figure 1:** Schematic greenhouse with porous vegetal stand

180

181 *2.5 Simulations*

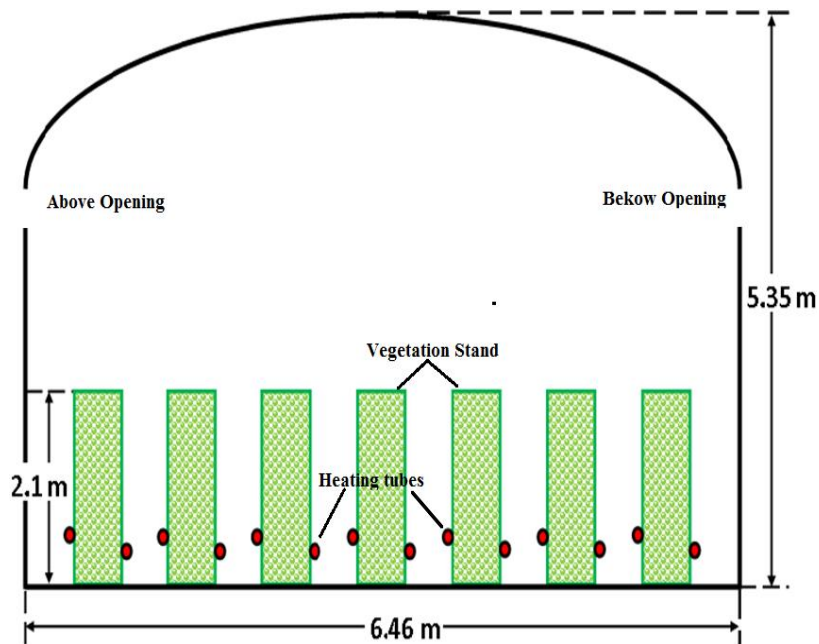
182

183 *2.5.1 Description of the problem studied*

184

185 The greenhouse geometry used for this study for simulations is of single chapel type with following
186 dimensions: 20 m long, 6.46 m wide and 5.35 m high (so that average inside volume estimated by CFD
code, $Vol = 560 \text{ m}^3$) as shown in Fig. 2. It has two channels with openings and its ventilation is performed

187 by adjustable openings placed laterally. The simulation was performed under the climate conditions of
 188 Tizi-Ouzou region ($36^{\circ} 47' 59''$ North latitude and $4^{\circ} 1' 59''$ East longitude). The heating of air inside
 189 the greenhouse is provided by hot water circulation, in tubes parallel to the vegetation rows, located 30
 190 cm above the ground (see Fig. 2). The rows were 2.1 m high, 0.7 m wide and are separated by aisles, 0.7
 191 m wide. The leaf area index LAI_S (m^2_{leaf}/m^2_{soil}) is estimated to value 3. The vegetation is considered in
 192 that case as well of heat and source of water vapor.
 193



194
 195 **Figure 2:** Schematic vegetal stand with heating tubes

196 2.5.2 Boundary conditions

197 The boundary conditions (see fig.3) used for this study are:

198 - For the external wind velocity, a logarithmic profile deduced from experimental measurement has
 199 been used to model the atmospheric wind velocity at the inlet boundary of the simulated domain,
 200 located from North (Haxaire, 1995). Hence, inlet velocity u_∞ has been defined as: $u_\infty =$
 201 $(u^*/K) \ln(z/z_0)$; with u^* , the friction velocity ($u^* = 0.28 \text{ m s}^{-1}$); K the Von Karman constant
 202 ($K = 0.41$) and z_0 the friction length ($z_0 = 0.0193 \text{ m}$).
 203 - Outside air temperature and absolute humidity are respectively defined as, $T_e = 14 \text{ }^{\circ}\text{C}$ and $w_e = 7.4$
 204 $\text{g}_v/\text{kg}_{\text{dryair}}$,
 205 - At the upper boundary layer, a differential pressure of zero was imposed,
 206 - For heat gain in greenhouse, the flux due to solar radiation received at the cover and restituted to
 207 the ambient air by convection, is estimated $17 \text{ } 100 \text{ W per m}^3$ of cover, for a global external
 208 radiation taken equal to $R_{ge} = 171 \text{ W m}^{-2}$, assuming that the convection term Φ_{conv} represents 6% of
 209 the outside radiation (Chemel, 2001[11]).

210 The convective flow reemitted from the soil to air ambient is estimated using the following equation:

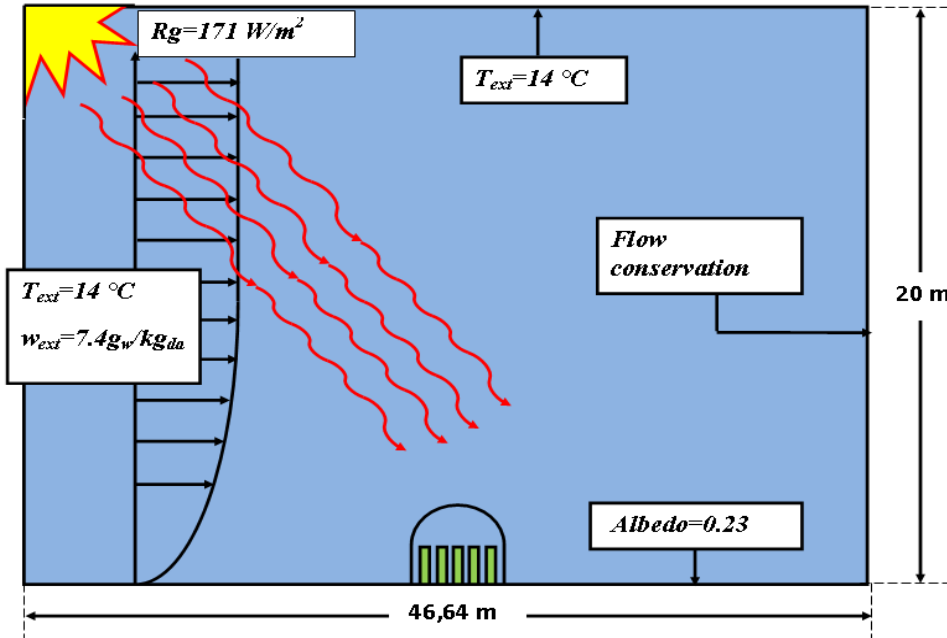
211

$$212 R_{sol} = R_s(1 - a) = R_{ge}(1 - a) \exp(-k_c LAI_S/2) \quad (14)$$

213

214 Where R_s , represents the solar heat flow on the vegetation stand.

215 Solar irradiation received at the ground is estimated assuming that the vegetal covers all greenhouse soil
216 surfaces but the height is only half of its real value. For this vegetal cover, the albedo equals 0.23 and the
217 heat flow exchanged with inside air is estimated at a reasonable value of 27 W.m^{-2} .



234 **Figure 3:** Outside boundary conditions for simulations

235 **3. Results and discussion**

236 The simulations were done for different opening windows at inlet and outlet of greenhouse and the
237 results permit us to obtain the following dynamic and thermal fields:

238 **3.1 Case of an unheated greenhouse**

239 **3.1.1 Velocity fields**

240 Near the opening, both at above as below, the air velocities are higher outside than inside vegetation
241 stand. In the picture shown in Fig. 4, we can observe one buckle of air recirculation inside the greenhouse,
242 creating then a vortex which changes in position and diameter for each opening. The inside air velocity
243 increase with the dimension of the opening. The maximum of the velocity is obtained at the top of the
244 chapel.

245

246

247

248

249

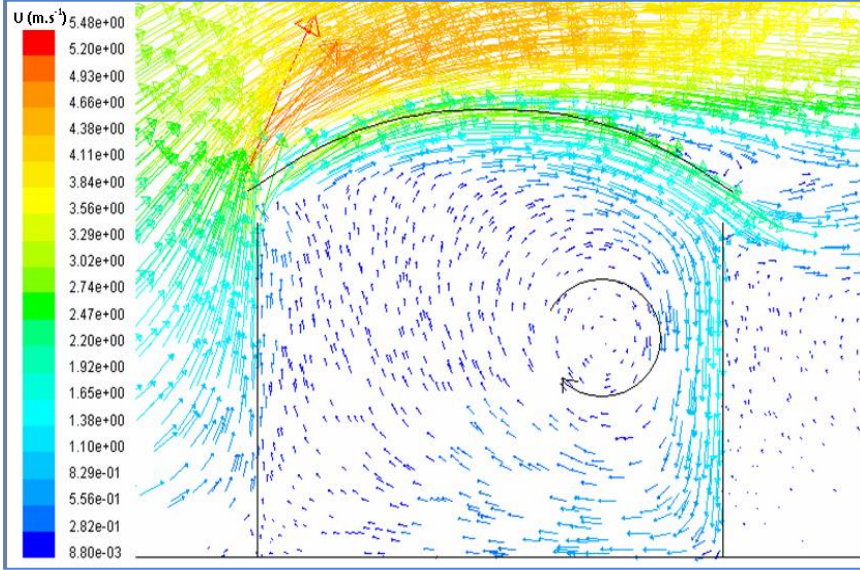
250

251

252

253

254



255
256
257
258
259
260
261
262
263
264
265
266
267
268 Figure 4: Velocity fields versus air renewal rate ($N = 21 \text{ Vol.h}^{-1}$, so opening 40/40 cm)
269
270

3.1.2 Temperature and humidity fields

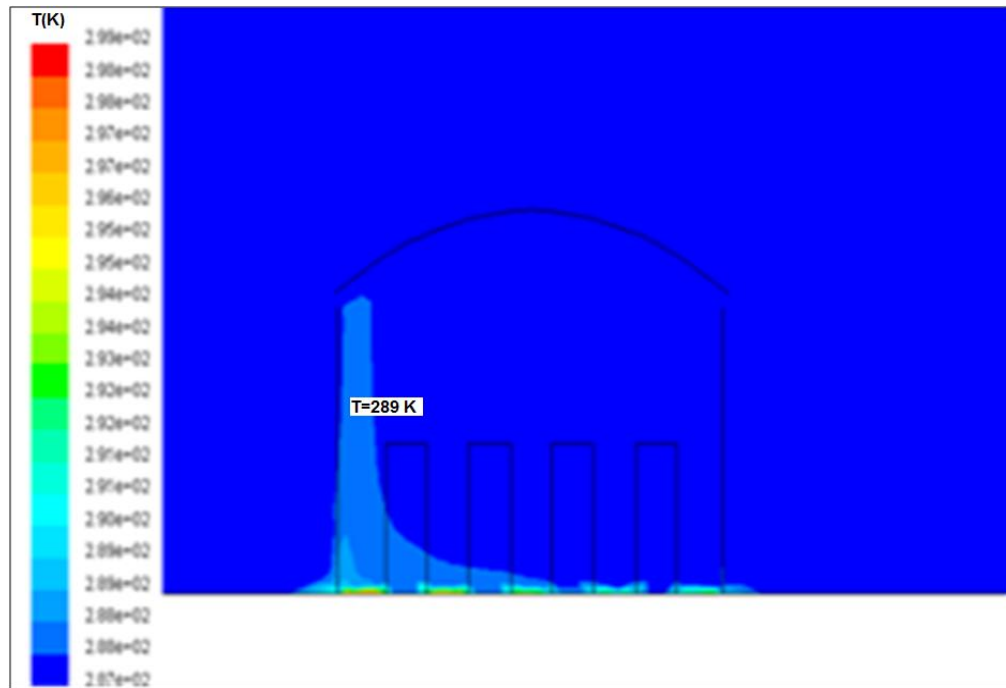
271 The illustration shown in the following pictures (see Figs. 5 and 6) reveals the heterogeneity of the
272 inside temperature and humidity. Air temperature is higher in the greenhouse wedges, sheltered from the
273 ventilation. Indeed, these zones are less ventilated, as the case of the part of soil surface situated between
274 the rows of vegetation. These zones are apart from that the most heated parcels because they receive
275 direct solar flux at midday (see fig. 5). Several tests of opening cases were simulated under the same
276 conditions for external air ($T_e = 14^\circ\text{C}$, $w_e = 7.4 \text{ g/kg}_{\text{dryair}}$).

277 To calculate the exchange rate N (Vol/h) the following expression (T. Boulard et al 1995[12]) is used:
278

$$279 \quad N = 3600 \frac{G_m}{\rho_a} V_{ol} \quad (15)$$

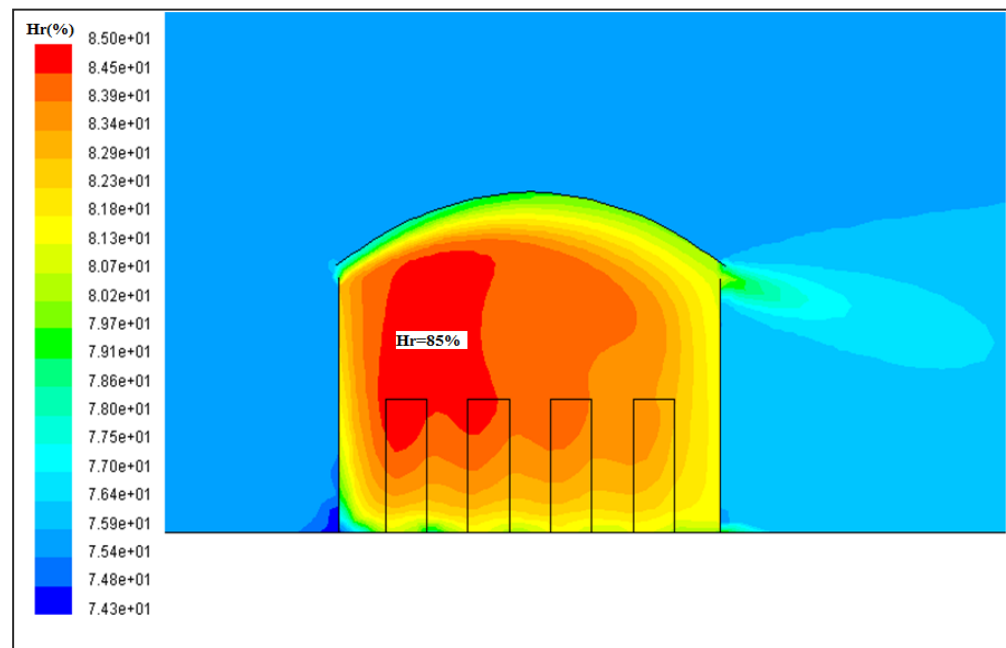
280

281 Where G_m (kg s^{-1}) is the air mass flux through the openings (with the hypothesis of mass
282 conservation) and Vol is the inside volume of greenhouse, estimated by CFD code at 560 m^3 .
283



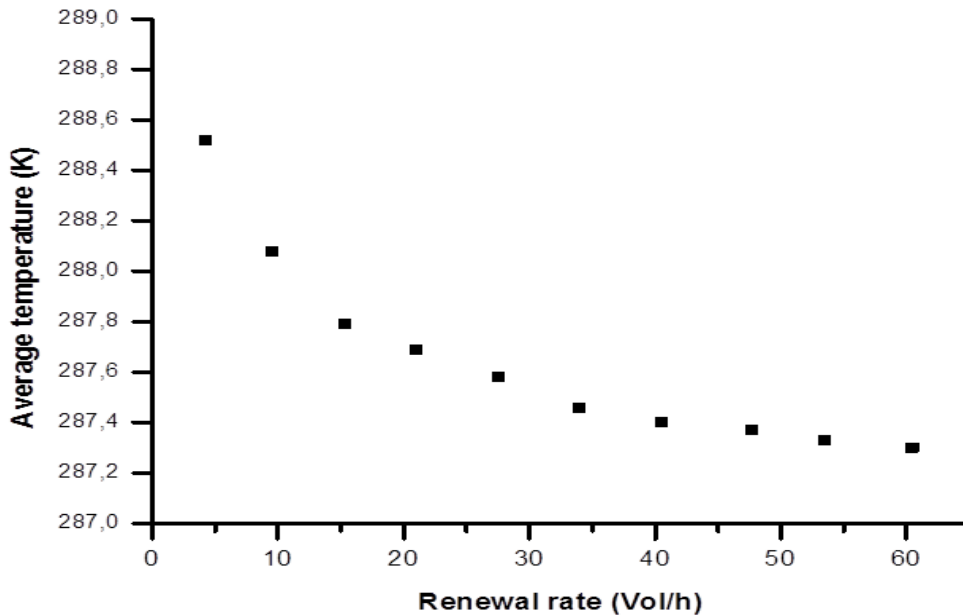
284
285 **Figure 5:** Temperature fields for unheated case ($N = 9.54 \text{ Vol.h}^{-1}$)
286

287 As shown in fig. 6, the maximal value of humidity ($H_r=85\%$) is obtained above the opening,
288 where the air velocity is lower. Near the ground, the humidity is stratified. It increases with the height of
289 vegetation.



290
291 **Figure 6:** Humidity fields for unheated case ($N=9.54 \text{ Vol.h}^{-1}$)

292 The simulations reveal that average internal temperature increases until 288.5 K when the exchange
293 rate decreases (see fig. 7) and for the large opening, corresponding to the high exchange rate, the average
294 temperature decreases progressively towards the value of the external temperature.



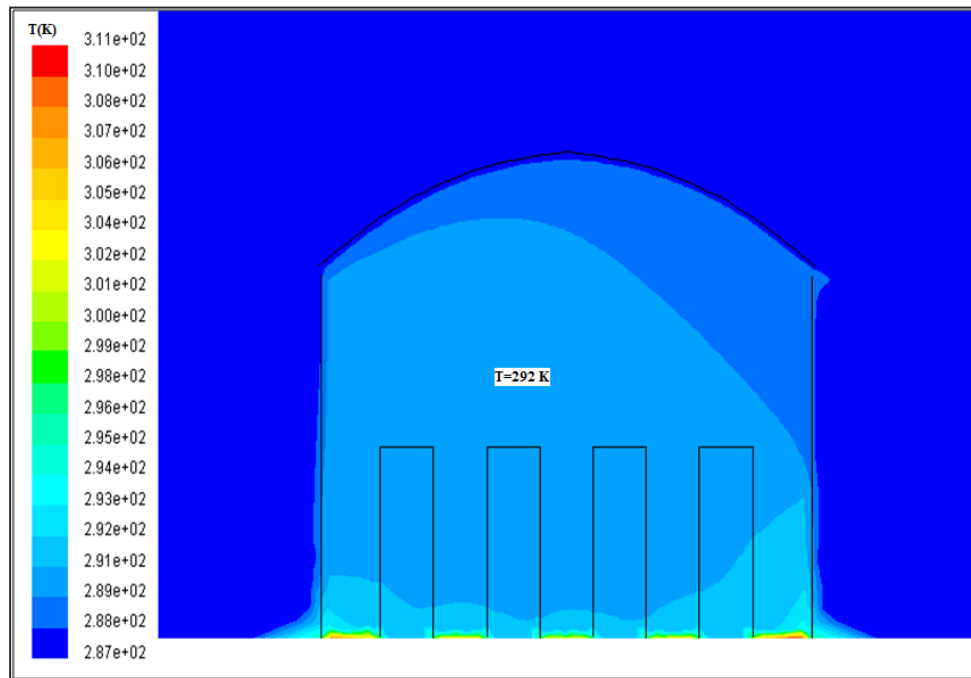
295
296

Figure 7: Inside average temperature

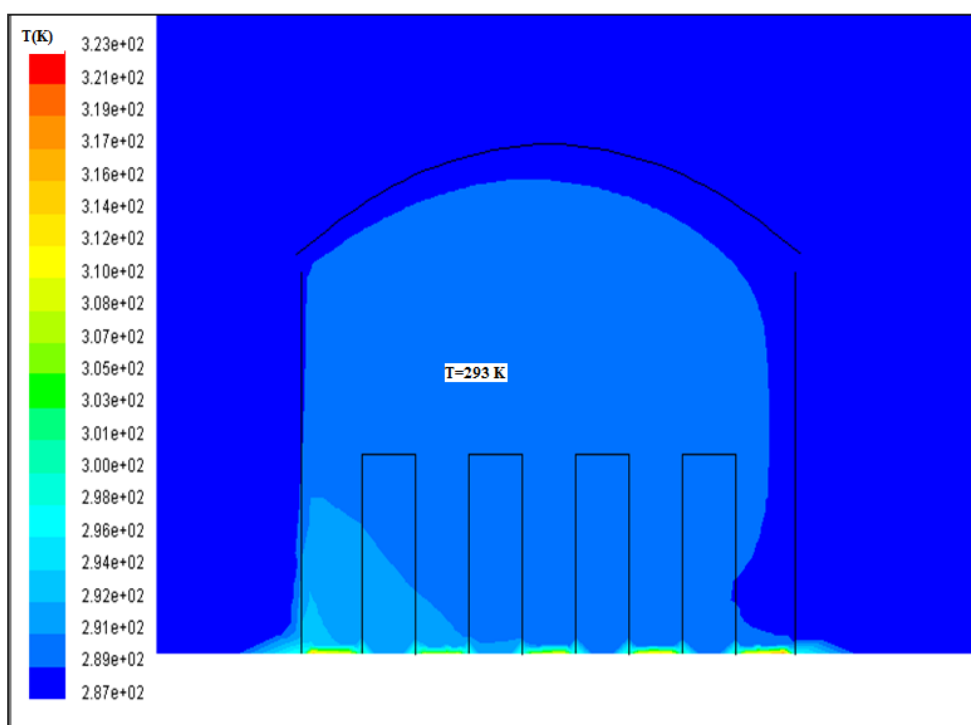
297 **3.2 Case of a heated greenhouse**

298 We keep the same climatic conditions than the precedent cases and we simulate for the openings of 10-10,
299 20-20, 30-30, 40-40, 50-50 and 60-60 cm. The inside temperature fields are simulated with heating
300 powers equal respectively to 75, 87, 100, 113 and 125 W m⁻² (applied for one m² of soil surface). The
301 obtained results are plotted in the **figs. 8, 9 and 10**. Near the ground surface, a significant temperature
302 gradient between soil and air can be noticed in the Fig.8, at the lower opening. But, with the large opening,
303 the temperature gradient between vegetation and air becomes insignificant, especially if the heating flux
304 is more important. In this case, the effect on air humidity will be benefic.

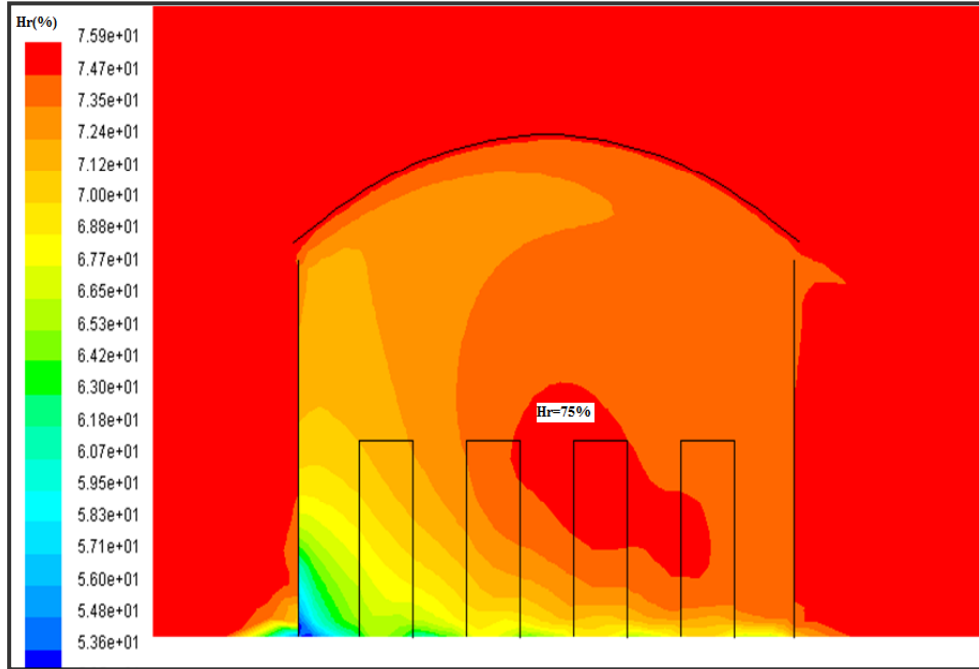
305



306
307 **Figure. 8:** Temperature fields versus air renewal rate ($N=4.5 \text{ Vol.h}^{-1}$, so opening 10/10cm, $HP=75 \text{ W.m}^{-2}$)
308



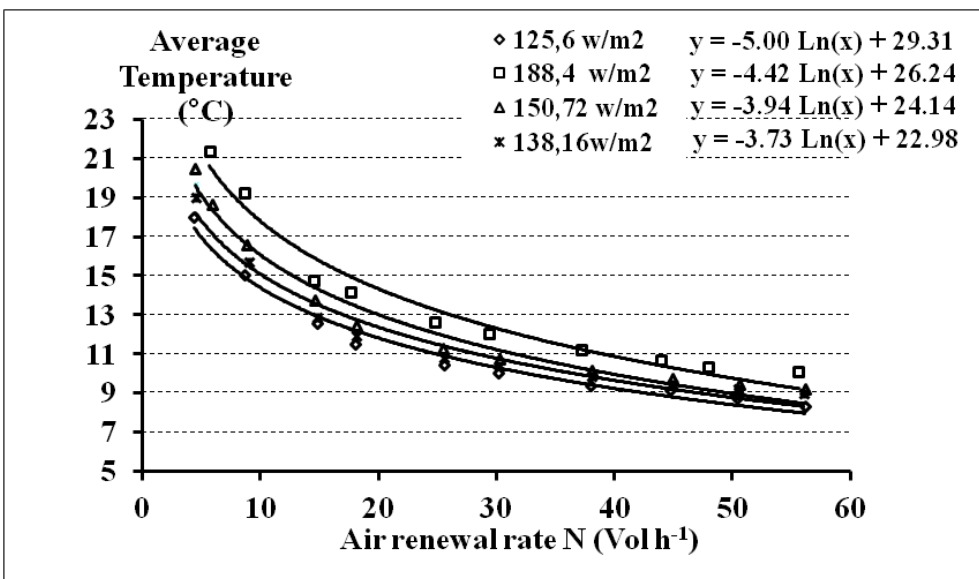
309
310 **Figure. 9:** Temperature fields versus air renewal rate ($N=8.42 \text{ Vol.h}^{-1}$, so opening 20/20cm, $HP=125 \text{ W.m}^{-2}$)
311
312



313
314
315
316
317
318

Figure 10: Inside humidity in a heated case ($N=8.42 \text{ Vol.h}^{-1}$; $HP=125 \text{ W.m}^{-2}$)

Thus, for heating powers respectively of 125, 138, 150 and 188 W.m^{-2} , we can plot the average temperature versus renewal rate (see fig. 11):



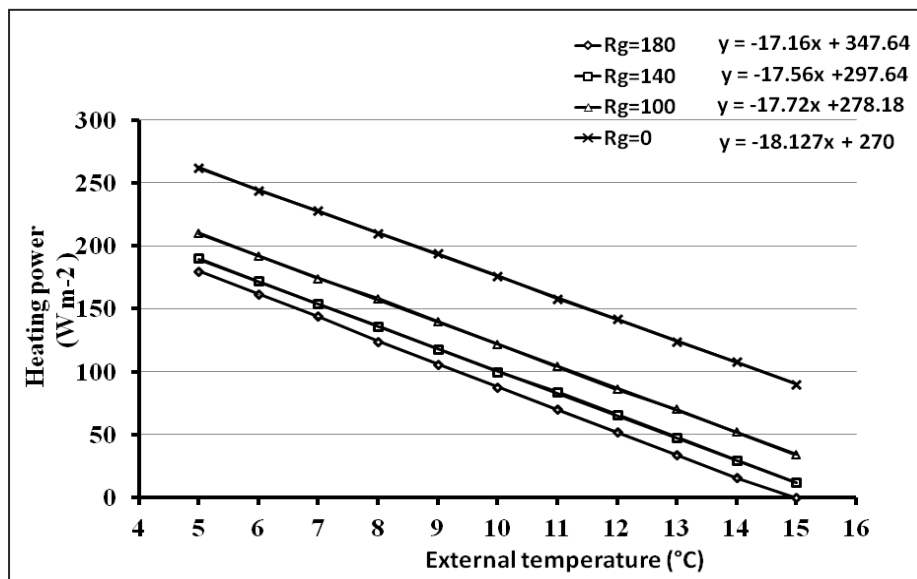
319
320
321
322
323

Figure 11: Average inside temperature versus renewal rate

Several tests of simulation were conducted with external conditions especially with the extreme case, where the external temperature equals the lower average level (minimal average temperature during 10

324 years). The evolution of temperature and humidity in greenhouse, versus heating power permits us to get
 325 the minimal heat power to be used for realizing the ideal conditions for the plant growing.

326 To understand more the phenomena and complete this study, we used an analytical program written in
 327 PASCAL code. It firstly consists in optimizing the heating-ventilation. In other terms, it is the search for a
 328 compromise between the heat power and the exchange rate, for different external conditions (global
 329 irradiation, temperature, relative humidity, etc.). The adopted strategy is to look for optimal temperature
 330 and relative humidity of ambient air necessary to insure the best development of plants. The software
 331 involves several number constants, few usual functions and various data to be introduced in the
 332 calculation, as external temperature, consign temperature of ambient air, global external irradiation,
 333 relative external humidity and relative consign humidity. The simulate conditions for the treated cases are
 334 given in the table 1. The external relative humidity was fixed at 50%, 60%, 70% and at 80%, and external
 335 air temperature was changed from 5 °C to 15 °C as inlet conditions for the program. We maintained the
 336 temperature less than 16 °C and we adjusted the internal relative humidity, Hr_a , to 80% as soon as
 337 possible. For each case, we looked for the necessary heating power as soon as possible and exchange rate
 338 required to realize these consign conditions of internal climate (16 °C, 80 %); on these tables , we can
 339 also get the values of the vapor pressure.. In this situation, the calculation with analytical model gives
 340 irradiation flux at ground surface, $R_{sol} = 21 \text{ W m}^{-2}$, and a volumetric power heat at the cover estimated at
 341 13 750 W m⁻³. For different external climates, we get the necessary heating power, with these abacuses
 342 shown in **Fig. 12**.



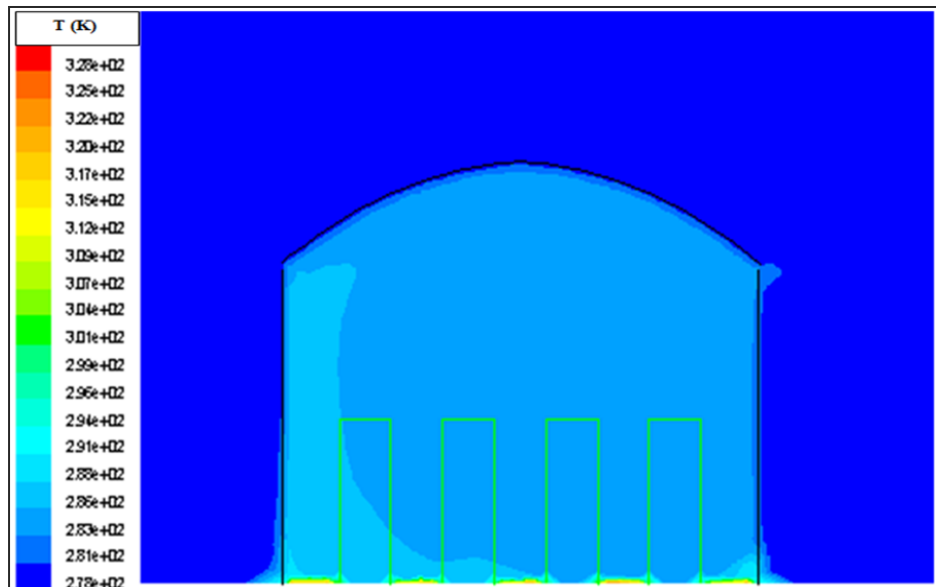
357 **Figure 12:** Heating Power versus external temperature
 358

359 These abacuses are more interesting because it permits to regulate the optimal heat power to use in
 360 order to ensure comfort temperature for plants, with exchange rate imposed by the needs of CO₂ for plants.
 361 This present study permits us to observe, with a good precision for different external conditions, the
 362 heterogeneity of the climatic variables and the moisture distribution of vegetal cover transpiration.

363 However, it does not inform in any case directly, about the heating ventilation phenomena. After several
364 tests of simulation, optimal cases are found (optimal heat power and exchange rate).

365 The main results of this present study are: i) the heating power does not depend or depends slightly on
366 external relative humidity, but it depends hardly of external temperature and global external solar
367 irradiation; ii) the exchange rate practiced does not depend on the external irradiation; iii) vegetal
368 temperature does not depend on external air humidity, its value increases with external solar irradiation.
369 All these results can be explained by the net irradiation flux intercepted by the plants. We can then notice
370 that the heating power is directly matched with external temperature, for different values of external solar
371 irradiation. These abacuses permit us to deduce, for each value of external global irradiation and external
372 temperature, heating power necessary to get the ambient air consign.

373 After the optimization of the precedent cases and keeping the same conditions, we complete this study
374 by the simulation, carried out with finite volume numerical method with Fluent® CFD code. For an
375 external temperature fixed at 5 °C and variable external irradiation, we fixed average internal temperature
376 at 16 °C and tried to reach 80 % of relative humidity. Then, we looked for air exchange rate and power to
377 be used. The results of these optimal cases are presented in figs.13 and 14. The simulation shows that the
378 obtained values of temperature and relative humidity are in a good agreement with the values obtained
379 with the analytical model.



395 **Figure 13:** Inside temperature in optimal case

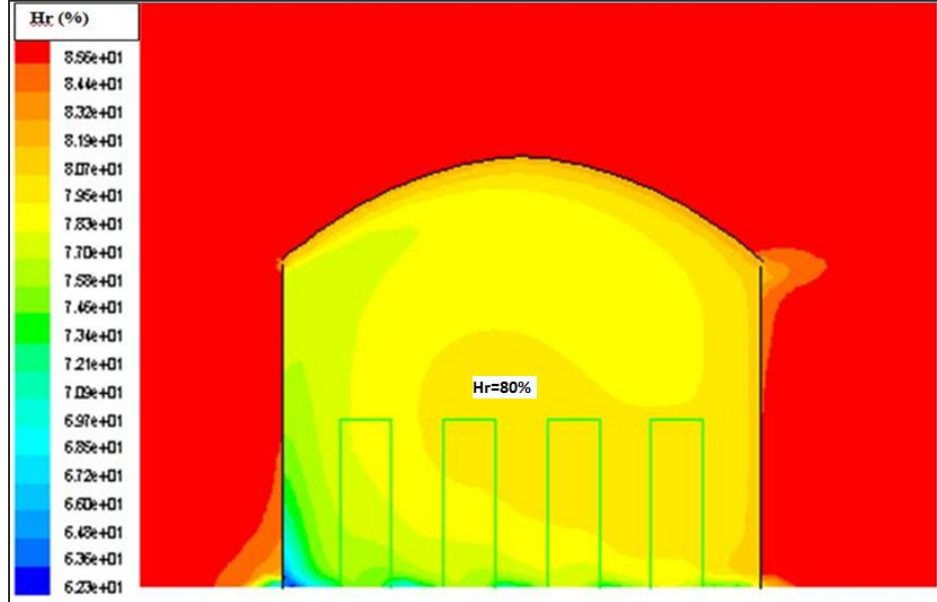


Figure 14: Inside humidity in optimal case

4. Conclusions

In the present study, the obtained abacuses associated with air humidity diagram, permit us to get a complete review of the features of internal air. The main result which can be exploited by the greenhouse users is the determination of the necessary heating power for each internal temperature and air relative humidity of consign, and its placement to insure the optimal conditions for a good development of plants , with air exchange rate corresponding to this fixed heating power. We can then predict the extreme cases in winter and predict the heating strategy in order to avoid all risks. This study needs however to be developed and completed with a series of measurements in greenhouse during the heating in winter season with different heat power and different openings.

Nomenclature

Symbols

a	Thermal diffusivity	$\text{m}^2 \text{s}^{-1}$
C	Volume sensitive heat	W m^{-3}
C_p	Specific heat at constant pressure	J kg K^{-1}
D	Diffusion coefficient	$\text{m}^2 \text{s}^{-1}$
E	Evaporation mass flux	$\text{kg m}^2 \text{s}^{-1}$
F	Volume force	m s^{-2}
h	Plant height	m
k_p	Intrinsic permeability	m
k	Turbulence kinetic energy	$\text{m}^2 \text{s}^{-2}$
k_C	Radiative extinction coefficient	

433	L_v	Latent vaporisation heat	J kg^{-1}
434	LAI_v	Volumetric folial indice	$\text{m}^2_{\text{vegetal}} \text{m}^{-3}$
435	P	Pressure	Pa
436	q	Internal heat source	W m^{-3}
437	R_{ge}	Global density flux	W m^{-2}
438	S	Surface	m^2
439	$S_{\Phi, P}$	Water source term	$\text{kg}_{\text{eau}}/\text{kg}_{\text{dry air}} \text{s}^{-1}$
440	t	Time	s
441	T	Temperature	K

442 **Greek symbols**

443	λ	Thermal conductivity	W m K^{-1}
444	ρ	Volumetric mass	kg m^{-3}
445	ω	Absolute humidity	$\text{kg}_{\text{eau}}/\text{kg}_{\text{air sec}}$
446	ν	Kinematic viscosity	$\text{m}^2 \text{s}^{-1}$
447	ε	Rate kinetic energy dissipative	$\text{kg m}^{-1} \text{s}^{-2}$

448

449 **References**

1. Haxaire, R. (1999). *Caractérisation et modélisation des écoulements d'air dans une serre*. Thèse de doctorat, Université de Nice Sophia Antipolis.
2. Bournet, P.-E., & Boulard, T. (2010). Effect of ventilator configuration on the distributed climate of greenhouses: a review of experimental and CFD studies. **Computers and Electronics in Agriculture**, **74**(2), 195–217. DOI: 10.1016/j.compag.2010.08.007
3. Roy, J. C., *et al.* (2002). Two-dimensional numerical simulation of natural ventilation in a multi-span greenhouse. **Biosystems Engineering**, **83**, 1–20.
4. Lee, I.-B., & Short, T. H. (2000). Convective and ventilation transfers in greenhouse. **Transactions of the ASAE**, **43**(3), 745–753. DOI: 10.13031/2013.2758
5. Villagrán, E. A., Baeza Romero, E. J., & Bojacá, C. R. (2019). Transient CFD analysis of the natural ventilation of three types of greenhouses used for agricultural production in a tropical mountain climate. **Biosystems Engineering**, **188**, 288–304. DOI: 10.1016/j.biosystemseng.2019.10.026
6. Ghernaout, B., Bouabdallah, S., Atia, A., & Arici, M. (2021). Heat and fluid flow in an open agricultural greenhouse in presence of plants. **Applied Mathematical Modelling and Applications**, **4** (February), 1–8. DOI: 10.18280/ama_b.641-401
7. Zhang, J., Zhao, S., Dai, A., Wang, P., Liu, Z., & Liang, B. (2022). Greenhouse natural ventilation models: how do we develop with Chinese greenhouses. **Agronomy**, **12**(9), Article 1995. DOI: 10.3390/agronomy12091995
8. Boulard, T., Kittas, C., Roy, J. C., & Wang, S. (2002). Convective and ventilation transfers in greenhouses, part 2: determination of the greenhouse distributed climate. **Biosystems Engineering**, **83**, 1–20.

470 9. Boulard, T., & Baille, A. (1993). A simple greenhouse climate control model incorporating effects of venti-
471 lation and evaporative cooling. **Agricultural and Forest Meteorology**, **65**, 1–20.

472 10. Nebbali, R., Roy, J. C., Boulard, T., & Makhlof, S. (2006). Comparison of the accuracy of different CFD
473 turbulence models for the prediction of the climatic parameters in a tunnel greenhouse. **Acta Horticulturae**,
474 **719**, 287–294.

475 11. Chemel, C. (2001). *Modélisation et simulation des écoulements d'air dans les serres*. Thèse de maîtrise de
476 mécanique, INRA, Avignon, France.

477 12. Boulard, T., & Baille, A. (1995). Modeling of air exchange rate in greenhouse equipped with continuous roof
478 vents. **Journal of Agricultural Engineering Research**, **61**(1), 37–47. DOI: 10.1006/jaer.1995.1028.

479

480

481

482

